Talanta 82 (2010) 25–33

Contents lists available at ScienceDirect

Talanta

journal homepage: www.elsevier.com/locate/talanta

A highly sensitive non-enzymatic glucose sensor based on a simple two-step electrodeposition of cupric oxide (CuO) nanoparticles onto multi-walled carbon nanotube arrays

Jiang Yang[a], Liao-Chuan Jiang[b], Wei-De Zhang[b], Sundaram Gunasekaran[a,*]

[a] Department of Biological Systems Engineering, University of Wisconsin-Madison, 460 Henry Mall, Madison, WI 53706, USA
[b] Nanoscience Research Center, School of Chemistry & Chemical Engineering, South China University of Technology, Guangzhou 510630, People's Republic of China

ARTICLE INFO

Article history:
Received 29 January 2010
Received in revised form 20 March 2010
Accepted 22 March 2010
Available online 27 March 2010

Keywords:
Carbon nanotube
Cupric oxide
Electrodeposition
Glucose
Non-enzymatic sensor

ABSTRACT

A novel, stable and highly sensitive non-enzymatic glucose (Glc) sensor was developed using vertically well-aligned multi-walled carbon nanotubes array (MWCNTs) incorporated with cupric oxide (CuO) nanoparticles. The MWCNTs array was prepared by catalytic chemical vapor deposition on a tantalum (Ta) substrate, while a simple and rapid two-step electrodeposition technique was used to prepare the CuO–MWCNTs nanocomposite. First, Cu nanoparticles were deposited onto MWCNTs at constant potential and then they were oxidized into CuO by potential cycling. The electrocatalytic activity of CuO–MWCNTs array was investigated for Glc under alkaline conditions using cyclic voltammetry and chronoamperometry. The sensor exhibited a linear response up to 3 mM of Glc and sensitivity of 2190 $\mu A\,mM^{-1}\,cm^{-2}$, which is two to three orders of magnitude higher than that of most non-enzymatic Glc sensors reported in the literature. The sensor response time is less than 2 s and detection limit is 800 nM (at signal/noise = 3). When tested with human blood serum samples, the sensor exhibited high electrocatalytic activity, stability, fast response and good selectivity against common interfering species, suggesting its potential to be developed as a non-enzymatic Glc sensor.

1. Introduction

Diabetes is a chronic disease causing metabolic and systemic disorders. With more than 220 million people affected, diabetes has become one of the major health afflictions worldwide, and the number of diabetes patients is expected to double in 20 years [1]. Therefore, it is of significant importance to develop fast, accurate and stable technologies to detect Glc levels, both *in vivo* and *in vitro* [2], not only in blood but also in other sources such as foods and pharmaceuticals. Clark and Updike developed the first enzyme electrode and amperometric enzymatic biosensors in the 1960s [3,4]. Since then electrochemical Glc sensors based on glucose oxidase (GOx) have been widely investigated owing to their high sensitivity, specificity, and low detection limit [5]. However, enzyme-based sensors involve complicated, multi-step immobilization procedures; and under critical operating conditions the measurements suffer from poor reproducibility, thermal and chemical instability, and high cost [6,7]. Environmental conditions such as temperature, pH, and humidity and the presence of ionic detergents and enzyme-poisoning molecules in the sample can easily affect the performance of GOx sensors [8]. As a result, there is an unmet need for a simple, stable, reliable, and sensitive sensor for direct non-enzymatic measurement of Glc level in blood and other samples.

Carbon nanotubes (CNTs) are popularly used in electrochemical studies due to their unique structural and physical properties. CNTs have high electrical conductivity, chemical stability, large surface area, high surface/volume ratio, high mechanical strength, and chemically modifiable surface [9]. There has been several efforts to fabricate nanosensors using CNTs with metals/metal oxides such as Cu [6], Ag [10], Pt [11], CuO [12], ZnO [13], RuO_2 [14] MnO_2 [15], and TiO_2 [16], using various fabrication techniques including sol–gel, electrodeposition and self-assembly. New types of nanocomposites, often with enhanced electrochemical activities, increased surface area, improved biocompatibility, and promoted electron transfer, will generally retain the properties of each precursor or generate a synergistic effect [16]. The p-type semiconductor CuO has been used in numerous applications such as catalysis, semiconductors, batteries, gas sensors, biosensors, field transistors. CuO nanospheres [17], nanorods [18], nanowires [12], nanospindles [19], and nanoflowers [20] have been synthesized and used as sensors. However, the synthesis of CuO is tedious and often involves surface immobilization. The electrodeposition method of creating CuO is a simpler and time-saving alternative.

* Corresponding author.
E-mail address: guna@wisc.edu (S. Gunasekaran).

0039-9140/$ – see front matter © 2010 Elsevier B.V. All rights reserved.
doi:10.1016/j.talanta.2010.03.047

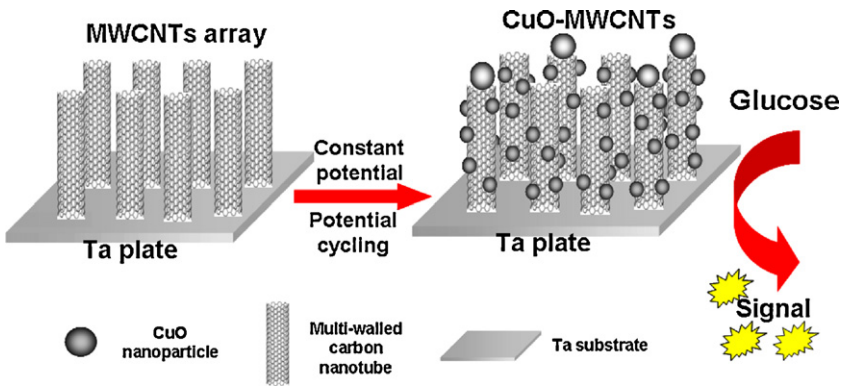

Scheme 1. A schematic diagram (not to scale) of the fabrication and application of CuO–MWCNTs Glc sensor. CuO nanoparticles are electrochemically deposited onto the MWCNTs array and the resulting nanocomposite generates electrochemical signals in the presence of Glc.

Herein we report a simple, two-step electrodeposition of CuO nanoparticles onto vertically well-aligned array of multi-walled CNTs (MWCNTs) as a biosensor for measuring blood Glc. Vertically well-aligned MWCNTs arrays were grown on Ta substrate via the catalytic vapor deposition technique [21] and Cu nanoparticles were then electrochemically deposited onto the MWCNTs array using the constant-potential film-plating technique (the first step) and oxidized *in situ* into CuO nanoparticles (the second step) by the cyclic potential sweep technique [22] (Scheme 1). The CuO-modified MWCNTs electrode was characterized by scanning electron microscopy (SEM), transmission electron microscopy (TEM), energy dispersive X-ray spectroscopy (EDS), X-ray diffraction (XRD) and electrochemical impedance spectroscopy (EIS). The CuO–MWCNTs electrode shows much higher sensitivity for Glc compared to the unmodified MWCNTs electrode and other non-enzymatic Glc sensors reported in the literature. This new CuO–MWCNTs nanocomposite material takes advantage of salient properties of both CuO and MWCNTs and promises to be an excellent non-enzymatic blood Glc sensor.

2. Experimental

2.1. Chemicals

D(+)-Glucose, L-ascorbic acid (AA), uric acid (UA), dopamine (DA), D-fructose, mannose, and lactose were purchased from Alfa Aesar. All other reagents were of analytical grade and were used as received without further purification. High quality deionized water (resistivity >18.4 MΩ cm^{-1}) was used for all experiments.

2.2. Apparatus

Electrochemical measurements were made using an electrochemical analyzer (CHI 660C, CH Instrument Inc., Shanghai, China). A conventional three-electrode system was used with a saturated Ag/AgCl (3 M KCl) reference electrode, a Pt wire counter electrode and the CuO/MWCNTs electrode that we developed. An unmodified MWCNTs array electrode was also used to compare with the performance of the CuO/MWCNTs electrode. All potentials were referenced to Ag/AgCl (3 M KCl) electrode.

EIS measurements were performed on a frequency response analyzer (PGSTAT 30, Autolab, Eco-Chemie, the Netherlands) with the same three-electrode configurations as above. A 100 mM KCl solution containing equimolar $[Fe(CN)_6]^{4-/3-}$ was used as the supporting electrolyte. Frequencies in the wide range of 0.1 Hz to 100 kHz were employed under open circuit potential conditions.

XRD patterns were recorded on an X-ray diffractometer (XD-3A, Shimadzu) with high-intensity Cu Kα radiation (λ = 1.5406 nm), at a scanning rate of 4° min^{-1} and a 2θ range from 20° to 100°. SEM and EDS were conducted (S-3700N, Hitachi) to observe the surface morphology of the CuO-modified vertically well-aligned MWCNT arrays and to analyze the surface elemental compositions during each step. TEM (H7650, Hitachi) was employed for the high-comparison and high-resolution analysis. Chemistry analyzer (Synchron CX9, Clinical System, Beckman, USA) was used in

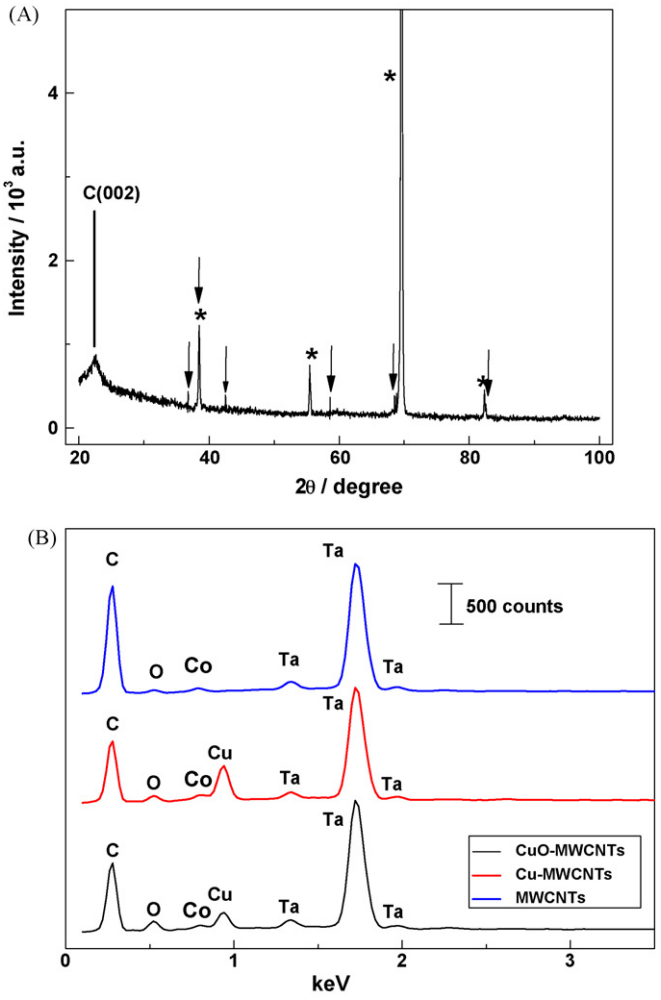

Fig. 1. (A) XRD pattern of CuO-modified well-aligned MWCNTs on a Ta substrate. Arrows indicate the reflections of CuO while stars indicate the reflections of Ta. (B) EDX analysis of different electrodes: unmodified well-aligned MWCNTs, Cu-MWCNTs and CuO–MWCNTs.

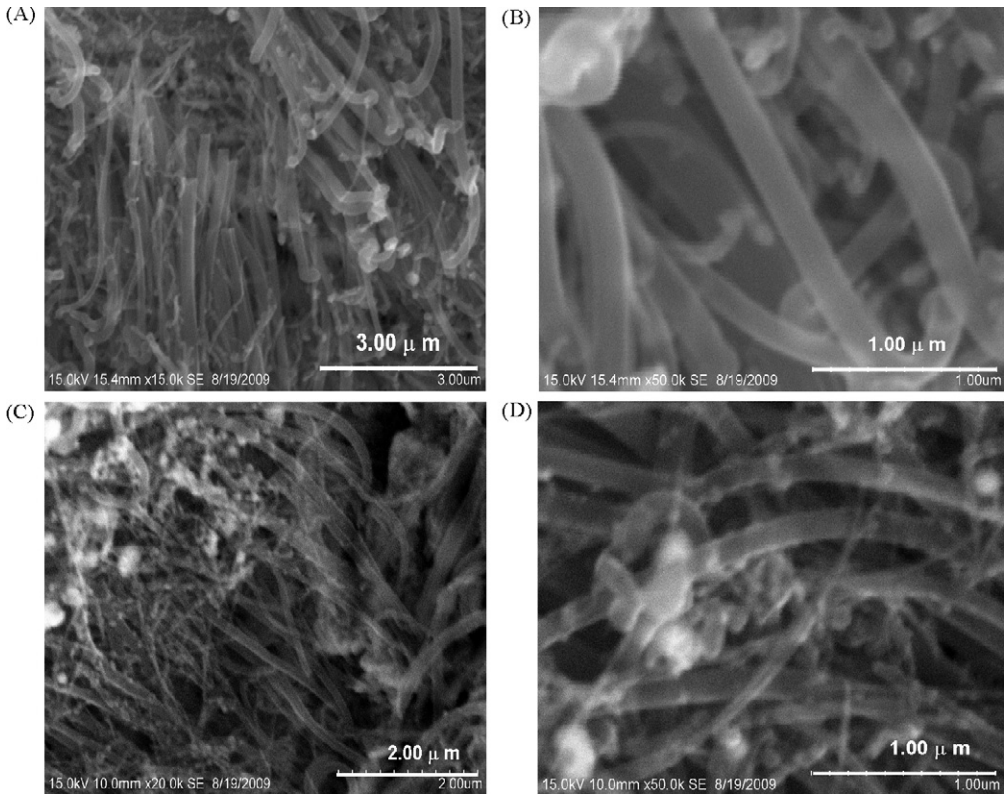

Fig. 2. SEM images of unmodified vertically well-aligned MWCNT array at low (A) and high (B) magnification, and CuO-modified MWCNTs at low (C) and high (D) magnification.

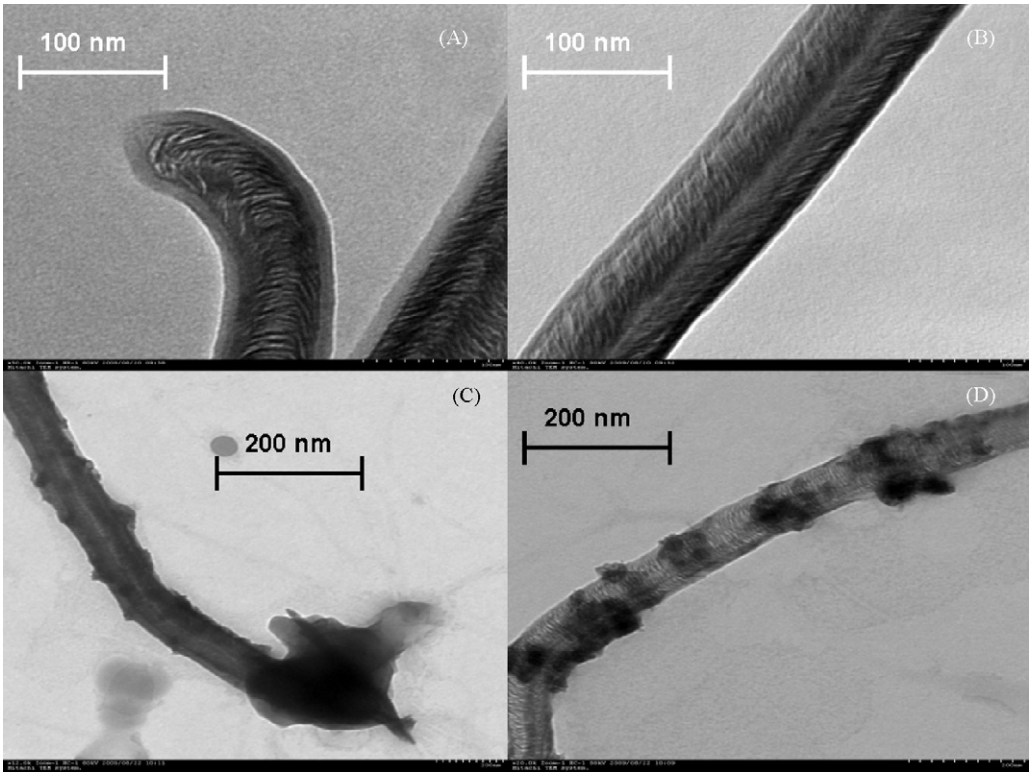

Fig. 3. TEM images of unmodified (A, B) and CuO-modified (C, D) MWCNTs.

the Nanfang Hospital affiliated with Southern Medical University (Guangzhou, China), to determine Glc contents in human blood serum samples within one hour after blood was drawn and to compare with the results of our sensor.

2.3. Preparation of the CuO/MWCNTs composite electrode

MWCNTs were grown on 3 mm × 3 mm Ta substrates by catalytic chemical vapor deposition technique [21,23]. Ta is an ideal substrate because it is chemically inert, highly conductive, and relatively inexpensive, with a high melting point enabling it to endure high temperature, which is required for growing MWCNTs. The Ta substrate with MWCNTs was fabricated as the MWCNT array electrode by connecting it to the surface of a GC electrode with a conductive silver paint (Structure Probe Inc., USA). The edges of the electrodes were insulated with nail enamel (Maybelline, USA).

As shown in Scheme 1, Cu nanoparticles were first electrochemically deposited onto the MWCNT array applying a constant potential; they were then oxidized into CuO by cyclic voltammetry (CV) [22]. Briefly, a constant potential of −0.40 V was applied to the MWCNT array electrode in a precursor solution of 100 mM KCl and 10 mM $CuCl_2$ which had been pre-purged with N_2 for 15 min. The best deposition time for this step was determined as 120 s. The electrode was then rinsed several times with water and dried with a flow of N_2 before it was repeatedly scanned in a 100 mM NaOH with CV under the potential range of −0.50 to 0.30 V at 100 mV s^{-1} for 20 cycles, allowing the Cu nanoparticles to be oxidized into CuO nanoparticles. The effective surface area of the CuO–MWCNTs electrode was estimated in a solution of 1 M KCl with 5 mM $K_3[Fe(CN)_6]$. The signal peaks were determined using the CHI 660C software coupled with the CHI electrochemical workstation. All experiments and measurements were performed at ambient temperature (25 ± 1 °C).

3. Results and discussion

3.1. Surface morphology

Fig. 1A shows the typical XRD patterns of the CuO–MWCNTs on Ta substrate. The reflections indicated by stars are indexed to Ta (JCPDS 4-788), while those indicated by arrows are to CuO, which are similar to the published data (JCPDS 65-2309 and JCPDS 44-0706). An obvious peak observed at $2\theta = 22.4^\circ$ is assigned to graphite carbon C(0 0 2) (JCPDS 75-1261). No typical peaks were observable for Cu or Cu_2O, indicating that the Cu deposited on MWCNTs was completely oxidized into CuO. EDS analysis further confirmed the elemental compositions at different steps (Fig. 1B). Ta substrate, O and a small amount of Co, used as the catalyst during MWCNT synthesis, were found in the unmodified MWCNTs. However, elemental Cu was only observed in the first and second steps, but absent in the unmodified MWCNTs. Moreover, the atomic ratio of O:Cu increased from 8.63 in the first step of constant-potential electrodeposition, to 60.26 after CV. This confirms Cu has been oxidized into CuO and successfully deposited onto MWCNTs.

A typical morphology of the unmodified MWCNTs array was studied by SEM. A vertically well-aligned array structure is easily seen in Fig. 2A and B. The sidewalls and tips of the unmodified MWCNTs are clean and relatively smooth; however, on the CuO–MWCNTs they are rougher and thicker with several granular CuO nanoparticles homogeneously attached on the surface (Fig. 2C and D).

The size and morphology of the unmodified MWCNTs and as-electrodeposited CuO–MWCNTs were further investigated by TEM. The tubular diameter of the unmodified MWCNTs array was 110.8 ± 5.5 nm (Fig. 3A and B, six measurements), compared to the values of 80–120 nm reported in the literature [24]. Consistent with SEM results, small and large CuO nanoparticles are observed on sidewalls and on tips of MWCNTs, respectively (Fig. 3C and D).

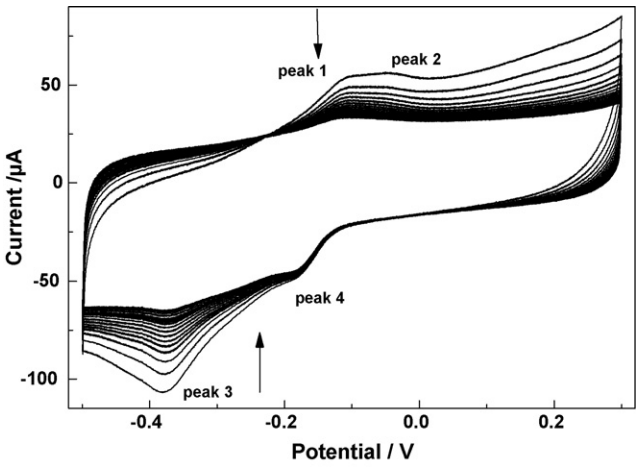

Fig. 4. Cyclic voltammograms of CuO–MWCNTs electrode in 100 mM NaOH at 100 mV s^{-1}. Arrows indicate the progression of the potential scanning (scanning range: −0.5 to +0.3 V).

3.2. Electrochemical characterization

The repetitive cyclic voltammograms for the electrochemical deposition of CuO nanoparticles onto MWCNTs with a supporting solution of 100 mM NaOH are shown in Fig. 4. The optimal number of cycles was determined to be 20 considering the catalytic levels (data not shown). There are two anodic peaks (peaks 1 and 2) and two cathodic peaks (peaks 3 and 4) in the scanning potential range. The anodic peaks (peak 1 and 2) in the range of −0.2 to 0.0 V are attributed to the oxidation of Cu_2O and CuOH to CuO while the cathodic peak between −0.3 and −0.4 V (peak 3) to the reduction of CuO into Cu_2O. This result is very similar to that of Le and Liu [22], who directly deposited CuO onto GC electrode surface. The cathodic peak around −0.2 V (peak 4) is due to the reduction of soluble O_2 by our as-synthesized MWCNTs array in the solution since the preparation of MWCNTs array involves N_2 [25]. During cyclic potential scanning, all redox peak currents decreased, suggesting CuO were formed during CV. The mechanism of the electrodeposition is shown below:

$$Cu + OH^- - e \leftrightarrow CuOH$$

$$2CuOH + OH^- \leftrightarrow Cu_2O + 2H_2O$$

$$Cu_2O + 2OH^- - 2e \leftrightarrow 2CuO + H_2O$$

EIS is widely used to study features of MWCNTs nanocomposite electrodes to obtain information on electron transfers between the electrolyte and the electrode surface. The Nyquist complex plane plot of the unmodified MWCNT array and CuO–MWCNT array electrodes in an electrolyte of 100 mM KCl and equimolar $[Fe(CN_6)^{4-/3-}]$ at the frequency range from 0.1 Hz to 100 kHz is shown in Fig. 5A. For MWCNTs the plot is nearly a straight line, which represents Warburg resistance and the diffusion-limiting step in the electrochemical process [26], whereas, for the CuO–MWCNTs nanocomposite electrode the plot is a straight line in the low frequency domain and a single semicircle in the high frequency domain. These illustrate that both diffusion-limiting and electron-transfer-limiting steps exist for CuO–MWCNTs. Also, the internal resistance of CuO–MWCNTs is lower than that of unmodified MWCNTs verifying that CuO acts as an electron mediator [14].

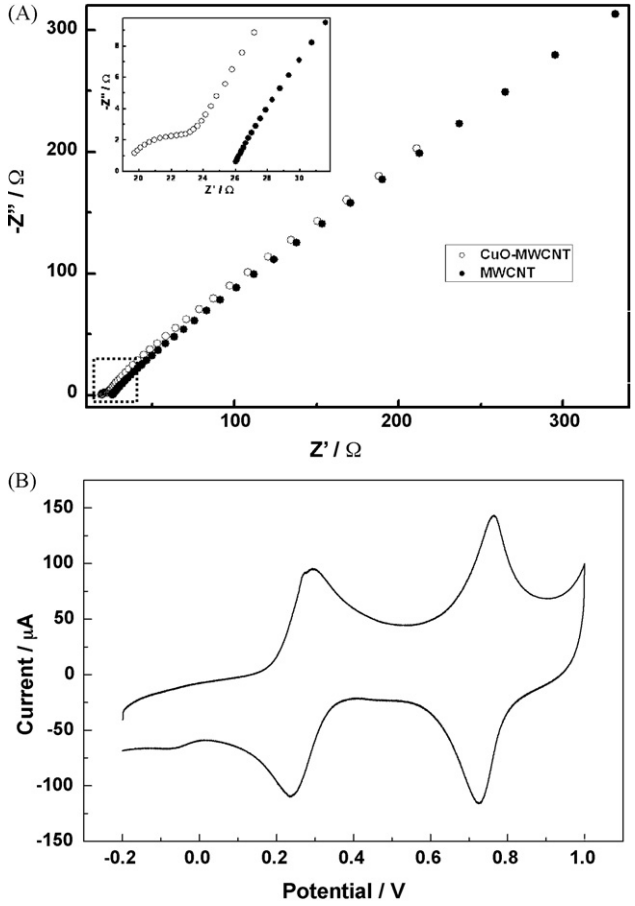

Fig. 5. (A) EIS of unmodified well-aligned MWCNTs and CuO–MWCNTs nanocomposite electrodes in 100 mM KCl electrolyte solution containing equimolar (0.01 M/0.01 M) $[Fe(CN)^6]^{4-/3-}$. The inset shows the magnification of the high frequency region. (B) Cyclic voltammograms of CuO–MWCNTs electrode in 5.00 mM $K_3[Fe(CN)_6]$ + 1.0 M KCl. (scanning range: −0.2 to 1.0 V).

In other words, the electron-transfer ability of MWCNTs array has been greatly improved by incorporating CuO nanoparticles.

To estimate the effective area of the CuO–MWCNTs electrode, a solution of 1 M KCl with 5 mM $K_3[Fe(CN)_6]$ was used. Fig. 5B is a typical cyclic voltammograms of the CuO–MWCNTs electrode at a scan rate of 100 mV s^{-1}. The pair of signature peaks from the redox reaction of $Fe(CN)_6^{3-}$ were found between +0.2 and +0.3 V, with a separation of peak potentials (ΔE_p) of 59 mV, indicating that the redox reaction is ideally reversible at the electrode after modification of CuO nanoparticles. Another pair of anodic and cathodic peaks, which is believed to be due to the redox reactions of deposited CuO, was found between +0.7 and +0.8 V corresponding well to the theoretical standard potential of CuO at +0.747 V. The redox reactions of CuO are as below [27]:

$$[Fe(CN)_6]^{3-} + 3H_2O \rightleftharpoons Fe(OH)_3 + 6CN^- + 3H+$$

$$2CuO + 2H^+ + 2e^- \rightleftharpoons Cu_2O + H_2O$$

For a reversible process under semi-infinite linear diffusion conditions at 25 °C, the effective surface area (A, cm^2) can be calculated in terms of peak current (I_p, μA) and scan rate (v, mV s^{-1}) according to the Randles–Sevcik equation:

$$I_p = 8.51 \times 10^{-3} * n^{3/2} A D^{1/2} v^{1/2} C$$

where n is number of electrons (=1), C is concentration (mM), D is diffusion coefficient (0.76×10^{-5} cm^2 s^{-1}). The calculated value of A was 0.076 cm^2 for the CuO–MWCNTs electrode, based on the redox peaks of $Fe(CN)_6^{3-}$.

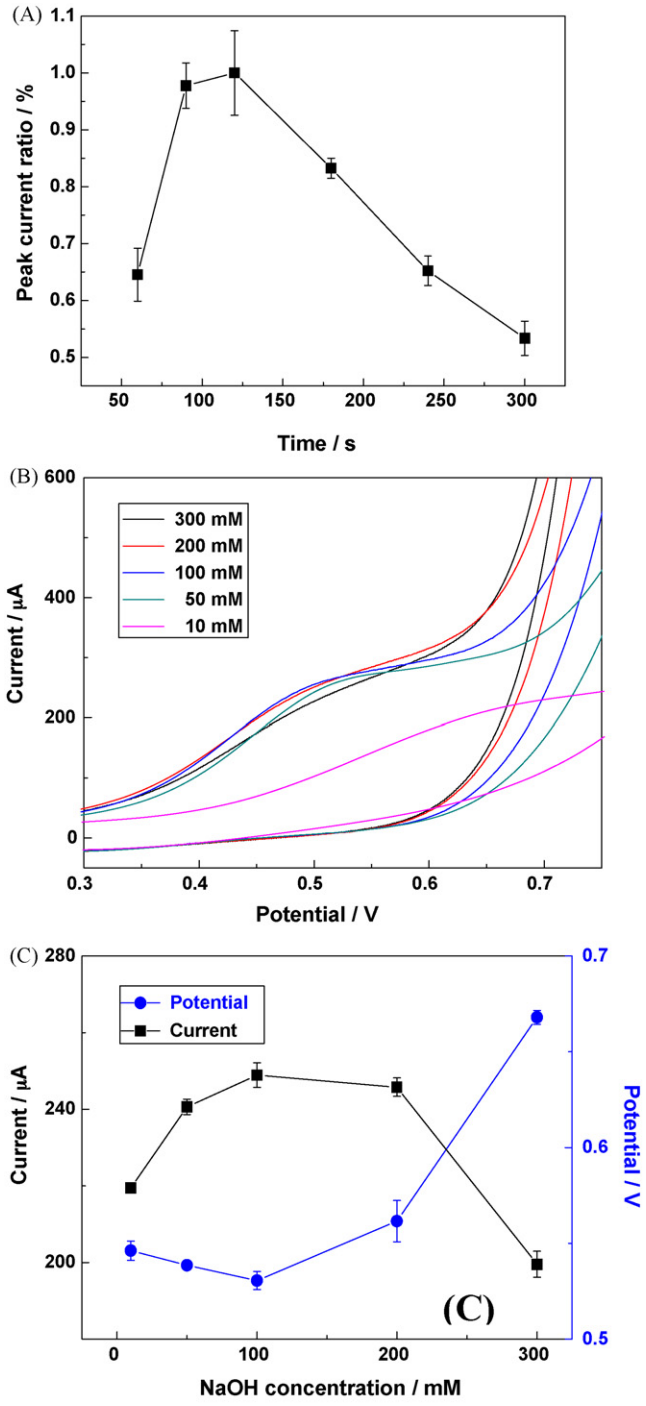

Fig. 6. (A) Effect of deposition time on peak current ratio (I/I_{max}). Error bars indicate the standard deviation of three measurements. (B) Cyclic voltammograms of 1.0 mM Glc in different NaOH concentrations at 100 mV s^{-1} (scanning range: 0–+0.8 V) (C) Effect of NaOH concentrations on peak current and peak potential to 1.0 mM Glc for the CuO–MWCNTs electrode.

3.3. Optimization for glucose sensing

Different durations of electrodeposition would result in different amounts of Cu nanoparticles being deposited onto MWCNTs, which would eventually generate different catalytic activities towards Glc for the CuO–MWCNTs composite electrode. Fig. 6A

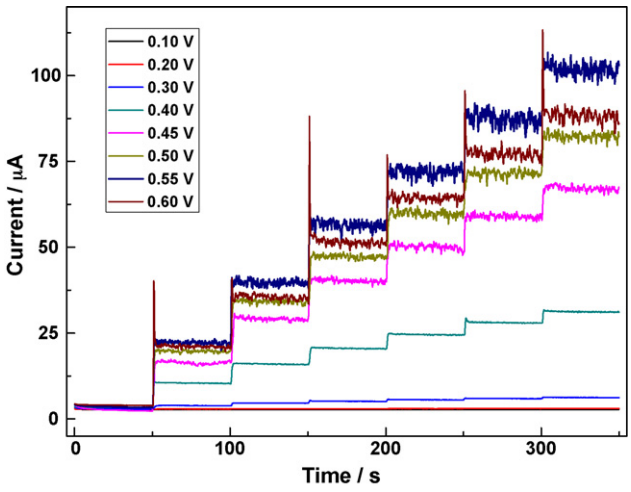

Fig. 7. Amperometric responses of CuO–MWCNTs electrode at different potentials in 100 mM NaOH with a dropwise addition of 0.1 mM Glc (applied potential: +0.10–+0.60 V).

shows the effect of the deposition time during the first step of synthesis under constant potential on the electrocatalytic activity of the nanocomposite electrode towards Glc oxidation. By examining the oxidation peak current ratio (I/I_{max}) for Glc, the optimal time was determined to be 120 s. MWCNTs could not be thoroughly covered by nanoparticles with a shorter deposition time, causing insufficient active sites for Glc catalysis. However, a longer deposition time causes the nanoparticles to aggregate into much larger particles or bundles, which negates the relative advantage of larger reactive surface area of smaller nanoparticles.

Since the catalytic reactions of Glc involve OH^- group, the pH would have a huge impact on the current and potential of Glc oxidation peaks in cyclic voltammograms. As shown in Fig. 6B and C, a series of NaOH solutions of different concentrations were used to study the pH effect on the oxidation of Glc at the CuO–MWCNTs electrode. The peak current first increased and then decreased when NaOH concentration was between 10 mM and 300 mM. The maximal peak current was when NaOH concentration was 100 mM. The peak potential remained steady for NaOH concentration between 10 and 100 mM, but increased with NaOH concentration (i.e., pH value) thereafter. Thus, larger potential should be applied at higher pH for maximal sensitivity. However, too high a potential and pH value would make many unrelated inteferents unstable and reactive in the test solution and generate many intermediate reactants that would probably interact with the electrode materials and hinder Glc reaction. Furthermore, such conditions might erode or harm the electrodes. Thus, 100 mM NaOH was selected as the optimal concentration to obtain the highest current at low potential.

Fig. 7 shows the amperometric responses measured to investigate the electroactivity of CuO–MWCNTs electrode towards dropwise addition of 0.1 mM Glc under different detecting potentials from +0.10 to +0.60 V in 100 mM NaOH. In general, the current response increased with the applied potential. The current response was really low at potentials lower than +0.30 V; it increased to about five-fold at +0.40 V while it reached the maximal value at +0.55 V, which even exceeded the current response at +0.6 V. This result is consistent with that of CV (Fig. 8A), which shows the anodic peak potential is at around +0.525 V. Therefore, +0.55 V was selected as the optimal constant detecting potential, not only because it generated a high enough signal but also because it was not unacceptably high. Relatively high potentials might

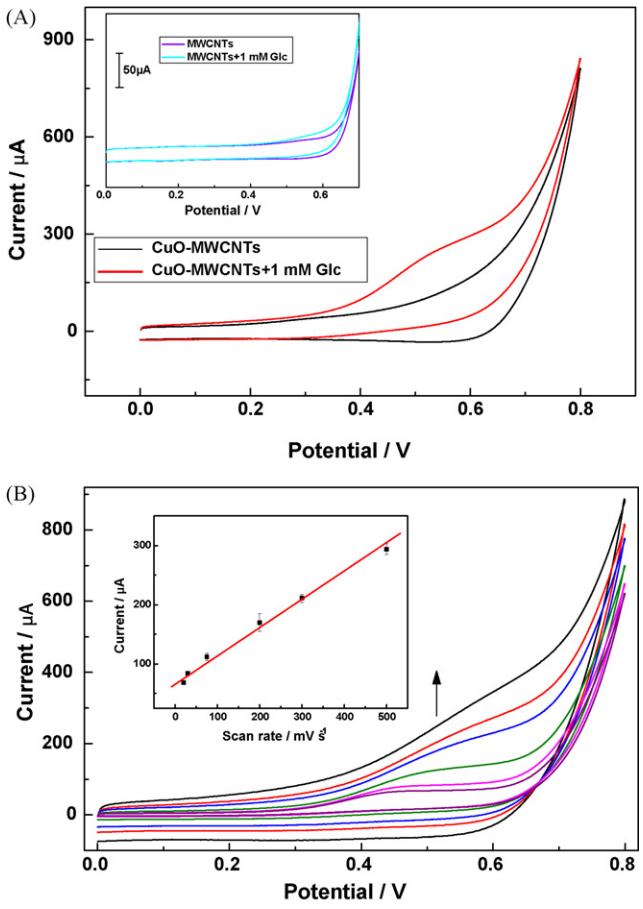

Fig. 8. (A) Cyclic voltammograms of MWCNT array electrode (Inset, scanning from +0.0 to +0.70 V) and CuO–MWCNTs electrode in 100 mM NaOH in the absence or presence of 1.0 mM Glucose at 100 mV s^{-1} (B) Cyclic voltammograms of CuO–MWCNTs electrode in 100 mM NaOH at different scan rate from 20 to 500 mV s^{-1}. The arrow indicates the increase of scan rates. Inset shows the oxidation peak current vs. scan rate (scanning range: 0–0.8 V). Error bars indicate standard deviations of three measurements.

oxidize some interfering species that are not reactive under low potentials.

3.4. Glucose sensing using cyclic voltammetry

The electrocatalytic activities of the unmodified MWCNTs electrode and the CuO–MWCNTs electrode were investigated using CV in 100 mM NaOH solution with and without 1.0 mM Glc at 100 mV s^{-1}, as shown in Fig. 8A. In the absence of Glc, neither the MWCNTs electrode nor the CuO–MWCNTs electrode shows oxidation peaks. When Glc was present, only a negligible response was sensed with the unmodified MWCNTs (Fig. 8A inset), which was possibly due to MWCNTs and maybe together with the minor contribution of remaining little amount of Co catalyst during the synthesis of MWCNTs array [28]. Such effects of metal or metal oxide impurities on MWCNTs have been attributed to electrochemical oxidation [29]. With Glc being added, a rapid increase in current, starting at about +0.35 V with the appearance of an obvious oxidation peak at around +0.55 V, showed up at the CuO–MWCNT electrode, indicating that CuO played a major role in the oxidation of Glc. The substantially higher current from the CuO–MWCNTs electrode than from the unmodified MWCNTs electrode in response to the Glc oxidation (Fig. 8A), is considered to be the result of a large surface area provided by MWCNTs arrays and the electrocatalytic active sites owing to the CuO nanostructures. Also, this

reaction at the electrode is completely irreversible as confirmed by the absence of a cathodic peak in the CV. All these results illustrate that the electrocatalytic performance towards the oxidation of Glc has been greatly improved by the electrodeposition of CuO nanoparticles onto the MWCNTs arrays.

The effects of different scan rates on the oxidation of Glc at the CuO–MWCNTs composite electrode in 100 mM NaOH using CV are shown in Fig. 8B. As the scan rate increased, the anodic peak current increased while the anodic peak potential shifted to a more positive region. A linear relationship between I_p and v was observed in the sweep range of 20–500 mV s^{-1} ($I_p = 70.71 + 0.4575^{*}v$; $R^2 = 0.996$), which illustrates that the electrochemical kinetics are controlled by surface adsorption of Glc molecules.

3.5. Amperometric responses of CuO–MWCNTs towards Glc

The amperometric responses of the unmodified and CuO-modified MWCNTs electrodes at a constant potential of +0.55 V to successive additions of 0.2 mM Glc in 100 mM NaOH are compared in Fig. 9A. Consistent with the results of CV (Fig. 8A), the CuO–MWCNTs electrode yielded a much larger current response than MWCNTs electrode. As observed in Fig. 9B, the current response of CuO–MWCNTs electrode exhibited a linear dependence on Glc concentration ($i(\mu A) = 35.31 + 166.51^{*}C$, $R^2 = 0.991$) with a very high sensitivity of 2190 μA mM^{-1} cm^{-2}. The upper Glc concentration limit for linear response was 3.0 mM and the detection limit was 800 nM (at signal/noise = 3). The performance of our CuO–MWCNTs sensor is compared with those of other published non-enzymatic Glc sensors in Table 1. The sensitivity of our sensor is substantially higher than that of other Glc sensors, about twice that of the next best sensor proposed by Lu et al. [30]; our sensor also boasts an excellent detection limit and linear range. This is owing to the nanocomposite nature of our CuO–MWCNT electrode based on MWCNTs, which facilitates high catalytic activity towards Glc and large active surface area.

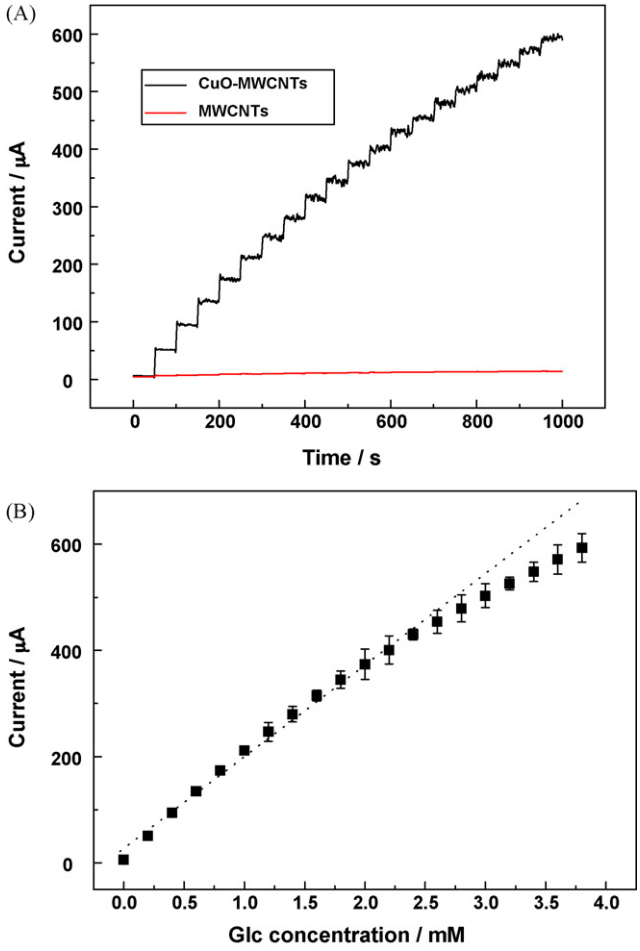

Fig. 9. (A) Current–time responses at +0.55 V with an increasing glucose concentration of 0.2 mM per 50 s for the MWCNTs array electrode and CuO–MWCNTs electrode (B) The dependence of the current response vs. Glc concentration at CuO–MWCNTs electrode. Error bars indicate standard deviations of three measurements.

3.6. Sensor stability and specificity

The stability of the sensor was investigated by measuring its sensitivity (S) over two weeks under ambient conditions during which the sensor retained 86.1% of its original sensitivity (S_o) (Fig. 10A). The CuO–MWCNTs response was stable over a long operational period of 50 min for 0.1 mM Glc in 100 mM NaOH with a loss of only 2.8% in the current signal (Fig. 10B). The current responses for 0.1 mM Glc were measured 10 times using the same electrode with only a relative standard deviation (RSD) of 3.6%. Three CuO–MWCNT electrodes fabricated under the same conditions had a RSD of 5.7%. These results confirm that the CuO–MWCNTs elec-

Table 1
Comparison of analytical performance of our proposed CuO–MWCNTs sensor with other published non-enzymatic glucose sensors.

Electrode type	Sensitivity (μA mM^{-1} or μA mM^{-1} cm^{-2})	Linear range (up to, mM)	Detection limit (μM)	Operational potential (V)
Pt nanotube array electrode [32]	0.1	14.0	1.0	+0.40
Mesoporous Pt electrode [33]	9.6	10.0	N/A	+0.40
Electrode based on bimetallic PtM (M = Ru, Pd and Au)-carbon nanotube-ionic liquid [34]	10.7	15.0	50.0	−0.10
Porous Au electrode [35]	11.8	10.0	5.0	+0.35
Pt-Pb alloy nanoparticles/MWCNTs [36]	17.8	11.0	1.8	+0.30
Macroporous Pt electrode [37]	31.3	10.0	0.1	+0.50
3-D gold film electrode [38]	46.6	10.0	3.2	−0.30
Gold nanoparticles electrode [39]	179.0	8.0	0.05	+0.16
Cu nanocluster/MWCNTs/GC electrode [6]	253.0	3.5	0.21	+0.65
Gold nanowire array electrode [40]	309.0	10.0	50.0	−0.40
CuO nanorods–graphite electrode [41]	371.4	8.0	4.0	+0.60
CuO nanospheres electrode [17]	404.5	2.6	1.0	+0.60
Ni-carbon nanofiber paste electrode [42]	420.4	2.5	1.0	+0.60
Self-assembled CNT thin films with Cu nanoparticles electrode [7]	602.0	1.8	0.1	+0.55
CuO nanoflowers-graphite electrode [41]	709.5	N/A	4.0	+0.60
Ni nanowire array electrode [30]	1043	7.0	0.1	+0.55
CuO–MWCNTs array electrode [this paper]	2190	3.0	0.8	+0.55

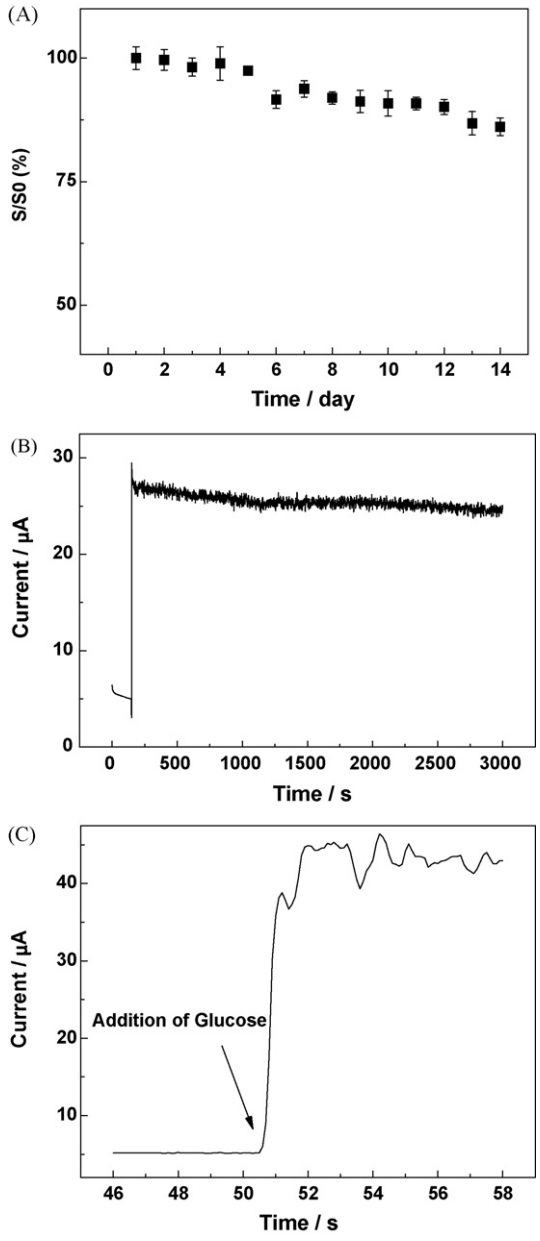

Fig. 10. (A) Stability of the sensor stored at ambient conditions over two weeks using 100 mM NaOH with 0.1 mM Glc at +0.55 V. (B) Chronoamperogram for 0.1 mM glucose in 100 mM NaOH at +0.55 V over a long period of operational time, 3000 s. (C) Response time of CuO–MWCNTs electrode to achieve steady-state currents.

trode has a high stability as well as good reproducibility that make it applicable for practical use.

The specificity of the sensor was investigated using different interferents that normally co-exist with Glc in human blood serum and other samples (Table 2). CuO can be electrochemically oxidized into strong oxidizing Cu(III) species such as CuOOH or $Cu(OH)_4^-$ that can induce the C–C bond cleavage of Glc in alkaline solutions [31], with a detectable current signal. The physiological Glc level is 3 to 8 mM while the other oxidizable interferents such as uric acid (UA), ascorbic acid (AA) and dopamine (DA) are present at levels as low as 0.1 mM, with a Glc:interferents ratio of more than 30:1. Besides, other carbohydrate compounds may also affect the performance of the sensor [18]. For all the co-existing interferents tested in 100 mM NaOH, CuO–MWCNTs electrode did not show any significant decline in the sensor response (Fig. 11), and the current responses due to the added interferents were only 0.14–3.44% as that of Glc (Table 2). The interferences we obtained for AA and UA were less than 1%, which is far lower than 27.0–28.5% Ye et al.

Table 2
Effect of interferents on glucose determination for the CuO–MWCNTs electrode.

Interferents	D(+)-Glucose:interferent molar ratio	Current ratio (%)
Dopamine	20:1	1.34
Ascorbic acid	20:1	0.89
Uric acid	20:1	0.98
Lactose	20:1	0.14
Mannose	20:1	1.66
Fructose	20:1	2.90
Citric acid	5:1	1.50
Sodium citrate	5:1	1.69
Potassium dihydrogen phosphate	5:1	3.44
Sodium chloride	5:1	1.60
Sodium benzoate	5:1	1.20

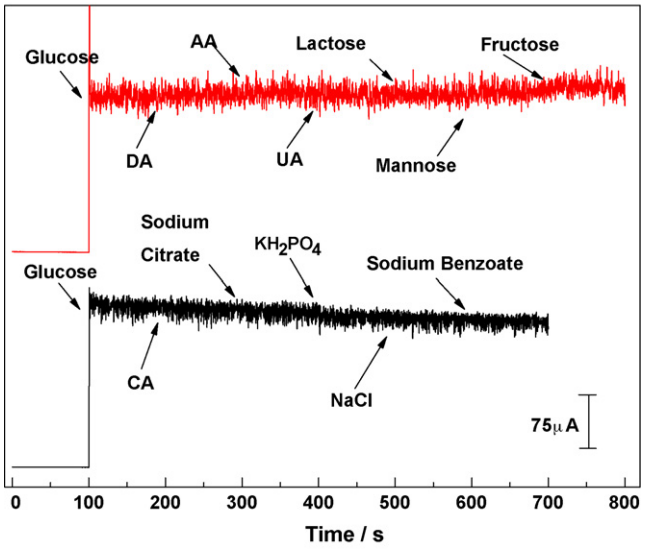

Fig. 11. Interference test of the sensor in 100 mM NaOH at +0.55 V with 0.1 mM glucose and other interferents as indicated.

Table 3
Determination of glucose in human blood serum samples.

Blood sample	Glc value measured with Beckman (mM)	CuO–MWCNTs sensor			
		Measured Glc value (mM)	RSD (%)	Added Glc (mM)	Recovery (%)
1	5.0	5.2	2.5	0.1	94
2	12.8[a]	12.9	4.0	0.1	96
3	4.6	4.5	3.2	0.1	102
4	5.2	5.4	4.7	0.1	97
5	4.9	5.0	2.9	0.1	94

[a] The person with the blood has already been diagnosed to be in diabetic conditions.

obtained using unmodified MWCNTs array electrode [28]. This is because, in alkaline solutions, DA and AA are easily oxidized. Therefore, they are unlikely to react with CuO and result in weak signals. As for UA, which is in the highest oxidation state, also with relatively stable N-containing aromatic ring structure, it is difficult to be oxidized by CuO. The results verified the high specificity of our sensor towards Glc in the presence of various organic and inorganic interferents. The chloride poisoning, which has been a major problem for most metal or metal oxide electrochemical Glc sensors [12,17] was not found in our study. Furthermore, the current response becomes stable in less than 2 s, which indicates a significantly rapid response of CuO–MWCNTs towards Glc (Fig. 10C).

The sensor also performed well against a Beckman instrument used in a hospital (Table 3) for measuring Glc concentrations in human blood serum. All tests were done within an hour after blood was drawn. 40 μL serum sample was added to a 10.0 mL 100 mM NaOH testing solution under the operation potential of +0.55 V. The CuO–MWCNTs sensor displayed results consistent with those of Beckman in the hospital (human blood serum samples and hospital results were provided by Nanfang Hospital, Guangzhou, China).

4. Conclusions

We successfully fabricated vertically well-aligned MWCNTs array and electrochemically deposited CuO nanoparticles onto the sidewalls and tips of MWCNTs by a simple, fast, and effective two-step electrodeposition method. The CuO-modified MWCNTs displayed substantially higher electrocatalytic activity to Glc oxidation with a higher current response and lower oxidation potential than the unmodified MWCNTs. This CuO–MWCNTs electrochemical sensor has a low detection limit of 800 nM and a very high sensitivity of 2190 $\mu A\,mM^{-1}\,cm^{-2}$, and its response is linear for up to 3.0 mM Glc concentration. When these superior performance characteristics are combined with ease of fabrication, long-term stability, good reproducibility, rapid response, and excellent specificity to Glc in the presence of common interferents, the CuO–MWCNTs electrode is a potential candidate for routine Glc analysis.

References

[1] WHO, Fact sheet No. 312 in World health Organization (2009).
[2] J. Wang, Chem. Rev. 108 (2008) 814.
[3] S.J. Updike, G.P. Hicks, Nature 214 (1967) 986.
[4] L.C. Clark, C. Lyons, Ann. NY Acad. Sci. 102 (1962) 29.
[5] T.W. Tsai, G. Heckert, L.F. Neves, Y.Q. Tan, D.Y. Kao, R.G. Harrison, D.E. Resasco, D.W. Schmidtke, Anal. Chem. 81 (2009) 7917.
[6] X.H. Kang, Z.B. Mai, X.Y. Zou, P.X. Cai, J.Y. Mo, Anal. Biochem. 363 (2007) 143.
[7] X. Li, Q.Y. Zhu, S.F. Tong, W. Wang, W.B. Song, Sens. Actuators B 136 (2009) 444.
[8] R. Wilson, A.P.F. Turner, Biosens. Bioelectron. 7 (1992) 165.
[9] A. Merkoci, M. Pumera, X. Llopis, B. Perez, M. del Valle, S. Alegret, Trends Anal. Chem. 24 (2005) 826.
[10] J.H. Lin, C.Y. He, Y. Zhao, S.S. Zhang, Sens. Actuators B 137 (2009) 768.
[11] L.Q. Rong, C. Yang, Q.Y. Qian, X.H. Xia, Talanta 72 (2007) 819.
[12] Z.J. Zhuang, X.D. Su, H.Y. Yuan, Q. Sun, D. Xiao, M.M.F. Choi, Analyst 133 (2008) 126.
[13] B. Fang, C.H. Zhang, W. Zhang, G.F. Wang, Electrochim. Acta 55 (2009) 178.
[14] J.S. Ye, H.F. Cui, X. Liu, T.M. Lim, W.D. Zhang, F.S. Sheu, Small 1 (2005) 560.
[15] J. Chen, W.D. Zhang, J.S. Ye, Electrochem. Commun. 10 (2008) 1268.
[16] L.C. Jiang, W.D. Zhang, Electroanalysis 21 (2009) 988.
[17] E. Reitz, W.Z. Jia, M. Gentile, Y. Wang, Y. Lei, Electroanalysis 20 (2008) 2482.
[18] C. Batchelor-McAuley, Y. Du, G.G. Wildgoose, R.G. Compton, Sens. Actuators B 135 (2008) 230.
[19] X.J. Zhang, G.F. Wang, X.W. Liu, J.J. Wu, M. Li, J. Gu, H. Liu, B. Fang, J. Phys. Chem. C 112 (2008) 16845.
[20] X.J. Zhang, A.X. Gu, G.F. Wang, W. Wang, H.Q. Wu, B. Fang, Chem. Lett. 38 (2009) 466.
[21] W.D. Zhang, J.T.L. Thong, W.C. Tjiu, L.M. Gan, Diamond Relat. Mater. 11 (2002) 1638.
[22] W.Z. Le, Y.Q. Liu, Sens. Actuators B 141 (2009) 147.
[23] W. De Zhang, Y. Wen, S.M. Liu, W.C. Tjiu, G.Q. Xu, L.M. Gan, Carbon 40 (2002) 1981.
[24] J.S. Ye, Y. Wen, W. De Zhang, L.M. Gan, G.Q. Xu, F.S. Sheu, Electroanalysis 15 (2003) 1693.
[25] K.P. Gong, F. Du, Z.H. Xia, M. Durstock, L.M. Dai, Science 323 (2009) 760.
[26] X.M. Ren, P.G. Pickup, J. Electroanal. Chem. 420 (1997) 251.
[27] M. Pourbaix, Atlas d'Equilibres Electrochimiques A 25 °C, Gauthiers-Villars et Cie, Paris, 1963.
[28] J.S. Ye, Y. Wen, W.D. Zhang, L.M. Gan, G.Q. Xu, F.S. Sheu, Electrochem. Commun. 6 (2004) 66.
[29] C.E. Banks, A. Crossley, C. Salter, S.J. Wilkins, R.G. Compton, Angew. Chem. Int. Ed. 45 (2006) 2533.
[30] L.M. Lu, L. Zhang, F.L. Qu, H.X. Lu, X.B. Zhang, Z.S. Wu, S.Y. Huan, Q.A. Wang, G.L. Shen, R.Q. Yu, Biosens. Bioelectron. 25 (2009) 218.
[31] H. Wei, J.J. Sun, L. Guo, X. Li, G.N. Chen, Chem. Commun. (2009) 2842.
[32] J.H. Yuan, K. Wang, X.H. Xia, Adv. Funct. Mater. 15 (2005) 803.
[33] S. Park, T.D. Chung, H.C. Kim, Anal. Chem. 75 (2003) 3046.
[34] F. Xiao, F.Q. Zhao, D.P. Mei, Z.R. Mo, B.Z. Zeng, Biosens. Bioelectron. 24 (2009) 3481.
[35] Y. Li, Y.Y. Song, C. Yang, X.H. Xia, Electrochem. Commun. 9 (2007) 981.
[36] H.F. Cui, J.S. Ye, W.D. Zhang, C.M. Li, J.H.T. Luong, F.S. Sheu, Anal. Chim. Acta 594 (2007) 175.
[37] Y.Y. Song, D. Zhang, W. Gao, X.H. Xia, Chem. Eur. J. 11 (2005) 2177.
[38] Y. Bai, W.W. Yang, Y. Sun, C.Q. Sun, Sens. Actuators B 134 (2008) 471.
[39] B.K. Jena, C.R. Raj, Chem. Eur. J. 12 (2006) 2702.
[40] S. Cherevko, C.H. Chung, Sens. Actuators B 142 (2009) 216.
[41] X. Wang, C. Hu, H. Liu, G. Du, X. He, Y. Xi, Sens. Actuators B 144 (2009) 220.
[42] Y. Liu, H. Teng, H.Q. Hou, T.Y. You, Biosens. Bioelectron. 24 (2009) 3329.